37 p

CAT. 30

USE OF DYNAMIC MODELS IN LAUNCH-VEHICLE DEVELOPMENT

By H. L. Runyan, H. G. Morgan, and J. S. Mixson

NASA Langley Research Center
Langley Station, Hampton, Va., U.S.A.

Presented at the
18th Meeting
Structures and Materials Panel - AGARD

Liege, Belgium
May 28, 1964

NATIONAL AERONAUTICS AND
SPACE ADMINISTRATION
WASHINGTON

USE OF DYNAMIC MODELS IN LAUNCH-VEHICLE DEVELOPMENT

By H. L. Runyan*, H. G. Morgan**, and J. S. Mixson***

NASA Langley Research Center

ABSTRACT

This paper discusses the role of reduced scale models in the solution of the structural dynamic problems of large launch vehicles. A general discussion of scaling principles is given followed by tabulation of the specific parameters for scaling of bending, longitudinal, and local vibrations; liquid sloshing; combined elastic-aerodynamic buffet; flutter; and ground wind phenomenon. Three examples of the use of models at Langley Research Center are presented illustrating the utility of reduced scale models.

INTRODUCTION

For many years models have played a vital role in the study and solution of a variety of problems in the fields of physics and engineering. It is the purpose of this paper to illustrate the latest use of model techniques for studying the structural dynamic problems of large launch vehicles. The type of model to be discussed herein is the physical model, usually of reduced size, having varying degrees of similarity to the full-scale flight hardware. Mathematical and electrical analog models, for example, will not be discussed.

The basic reasons for using models are the same for launch vehicles as they have been historically, that is, models provide a means whereby necessary data may be obtained with less expenditure of time, money, and effort than would be required for other means of data collection such as full-scale testing or calculations. The importance of models has increased, however, as new or more complex fields are entered, as the required data become more critical, and as the information obtainable by other means becomes less certain. For example, consider the phenomenon of buffet in relation to the restriction on structural weight of today's large space boosters. As structural weight is reduced to increase performance, the rigidity of structural members such as fairings and panels is reduced, thereby increasing the likelihood of large dynamic response. In these circumstances, model studies of these problems are often the best means of obtaining the required data.

The space age is a natural outgrowth of the aviation age. In the design and development of aircraft, model technology was reaching a very advanced stage. For instance, a flutter model of the research aircraft X-1E which contained a complete duplication of the control system, involving scaled linkage and damping

*Head of Structural Dynamics Branch.

**Head of Dynamic Response Section.

***Aerospace Engineer.

characteristics as well as the detailed wing elastic and dynamic properties was constructed several years ago at Langley Research Center. Industrial companies have successfully constructed and tested very detailed aeroelastic models of most of the current jet aircraft as well as scaled structural models of delta wings. Models have also been used for gust research, landing loads, dynamic stability, etc. Models were very extensively used in the design of the X-15 rocket aircraft and the success of this research airplane is due in part to the thorough model program.

Seemingly, with this large background of experience, extension to large boosters would have seemed natural. Except for aerodynamic tests on rigid models, the developed technology has not been extensively utilized. This may be attributed, in part, to the fact that many boosters were constructed under crash programs. The National Aeronautics and Space Administration is now becoming one of the major users of large boosters, and since many NASA launchings involve very expensive payloads and are limited in number, reliability has become an important consideration. In an effort to insure that the vehicles are reliable, models are playing an increasing role.

SYMBOLS

A	cross-sectional area, ft^2
a	longitudinal acceleration, ft/sec^2
E	Young's modulus, lb/ft^2
f	frequency, cps
G	torsion modulus, lb/ft^2
h	liquid depth, ft
I	cross-sectional moment of inertia, ft^4
I_α	mass moment of inertia per unit length, $slug\text{-}ft^2/ft$
I'	mass moment of inertia, $slug\text{-}ft^2$
K	shear constant
k	cross-sectional radius of gyration, ft
L	characteristic length, ft
M	mass, slugs
m	mass per unit length, slugs/ft

N_M Mach number

N_R Reynolds number

p internal pressure, lb/ft^2

r tank radius, ft

S_α static mass unbalance about e.a. per unit length, slug-ft/ft

t tank wall thickness, ft

V velocity, ft/sec

x_o elastic axis location, ft

ϵ surface roughness characteristic length, ft

μ liquid viscosity, slugs/ft-sec

ν Poisson's ratio

ρ density, $slugs/ft^3$

τ characteristic time, sec

ω circular frequency, radians/sec

ω_h circular bending frequency, radians/sec

ω_α circular torsion frequency, radians/sec

Subscripts:

l liquid

m model

p prototype

w tank wall

PROBLEM AREAS

A launch vehicle is a very efficient structure; as much as 90 percent of the weight at lift-off may be propellant, leaving only 10 percent for basic structure, propulsion, and payload. The vehicles are designed on the basis of strength with small factors of safety, and this design condition results in a

vehicle that has low relative stiffness. Consequently, the various dynamic problems are accentuated since the response is more a function of stiffness (EI) than strength.

In figure 1 is shown a schematic of a typical launch vehicle and a listing of some of the more important load sources. Discussing these loads from the time of flight aspect, the first major loading occurs while the vehicle is on the launch pad before engine ignition and is due to ground winds. These winds can impose large loads on the vehicle in the direction of the wind as a steady or oscillatory drag load. In addition, oscillatory loads in a direction normal to the wind direction may be imposed which are caused by the Karman vortex street or flow breakdown around the cylindrical shape. Due to engine ignition and launcher release, longitudinal oscillations may be induced which are important, both from a basic structural standpoint and from an equipment environment standpoint. This input may be particularly important for solid-propellant vehicles at ignition since the most efficient grain structure includes a chamber the length of the rocket stage and the sudden increase in pressure is felt by the complete stage. Also at engine ignition a high level of random vibration is produced which may be transmitted to the vehicle structurally or acoustically. These wind, longitudinal, and engine vibratory loads can also take important new forms if the vehicle is launched from a silo or underwater.

The most important flight regime from the standpoint of loads occurs during transonic flight and continues until the maximum dynamic pressure condition has been passed. During this phase of the flight there are a number of static and dynamic loading sources which are acting simultaneously. A large part of the load-carrying capability of the structure is required just to sustain the static loads, such as axial acceleration and aerodynamic drag. This makes the accurate determination of the dynamic loads, which are of concern in this paper, very important since only a small amount of structural capability remains after the static loads are imposed on the vehicle. Most important of the dynamic loads are probably those due to horizontal winds and wind gradients. Also, buffet loads arising from unusual payload shapes, protuberances, etc., can cause either a low-frequency excitation of the fundamental vehicle bending modes or a high-frequency excitation of equipment and local structure. At this same time, boundary-layer noise is building up and reaches a peak at maximum dynamic pressure.

Various stability problems may appear at various times during launch. Fuel slosh can occur any time during flight and is dependent on the configuration - in particular, the location of baffles. Of course, flutter is an always present phenomenon - both panel flutter and flutter of components such as fins. Still another type of instability which involves the automatic control system may exist. Even though the control system is capable of stabilizing the vehicle as a rigid body, a feedback involving flexibility can result in violent oscillations capable of destroying the vehicle. Therefore, for proper control system design as well as for dynamic response calculations, the vibration modes of the basic vehicle must be known. An illustration of a model for obtaining vibration modes of the Saturn booster will be given later.

Aerodynamic heating fortunately becomes significant late in the flight for the low acceleration vehicles normally used for space missions, when most of the

above problems are less serious. Thus, heating is more or less uncoupled from the problems which occur in the lower portion of the atmosphere.

GENERAL DISCUSSION OF SCALING

Models and dimensional analysis have been the subject of many excellent books and papers, for example, references 1 through 10. Therefore, in this paper no attempt will be made to develop the general theory of modeling. However, some remarks concerning scaling for structural dynamic problems of launch vehicles are in order.

Types of Models

Several classifications of models are possible. One such classification, from reference 5, divides models into four categories as follows:

I. True models

II. Adequate models

III. Distorted models

IV. Dissimilar models

The true model faithfully reproduces all significant characteristics of the prototype for which it is designed. The construction and testing of such a model is almost an impossibility for the complex interactions involved in launch-vehicle dynamics. Instead, most launch-vehicle dynamic models are in the second category of adequate models. As the name implies, such models give adequate or satisfactory predictions of vehicle characteristics under a specified set of conditions but may not completely satisfy all design specifications. For example, flutter models typically are designed to keep the Mach number the same between model and prototype but fail to satisfy Reynolds number specifications. If some of the design conditions are violated sufficiently to require correction of the predictions, the model is "distorted." Distorted models are often used where the variation of a parameter with size is well known. For example, material properties are known well enough that different materials may be used interchangeably and the results adjusted accordingly.

The final type is the dissimilar model. While it will not be discussed further in this paper, this is a very useful modeling concept in wide use. This is a model which bears no apparent resemblance to the prototype but, by analogy, gives results which can be related to the prototype. The obvious examples are the many structural dynamic problems which are studied by electrical-mathematical models on an analog computer.

Fundamental Units

The beginning of most scaling or modeling concepts is in a system of fundamental units. For launch-vehicle dynamic problems, three such units must normally be considered. A number of combinations of units exist but, for this class of problems, the M-L-T system (mass, length, and time) is usually most desirable. If heating of the structure is a factor in the problem being considered, a fourth unit, usually temperature, must also be included.

Dimensionless Ratios

A model will exhibit similitude to a prototype provided certain dimensionless ratios have the same values for both. These dimensionless ratios may be determined by a dimensional analysis of all quantities involved in the problem or from the differential equations which define the system. The well-known Pi-Theorem of Buckingham, reference 1, states that the number of these independent, dimensionless ratios which exists is equal to the difference between the total number of quantities involved in the problem and the number of fundamental units. For example, if eight quantities, such as frequency, pressure, viscosity, etc., are of importance in a problem wherein three fundamental units are required, five independent, dimensionless ratios can be formed from the eight quantities. A model of such a system would be similar to the prototype provided the five dimensionless ratios had the same value for both.

Scale Factors

To design a model to study some particular phenomenon, scale factors must be established for each of the quantities measured by the fundamental units. For example, these factors will relate mass, length, and time of the prototype to these same factors of the model. Choice of scale factors for a particular model will be influenced by such things as economy, available test facility capabilities, manufacturing tolerances, and instrumentation accuracies, but their relationship to one another must keep the values of the pertinent dimensionless ratios the same for model and prototype. For example, a length scale factor may be established by an available wind-tunnel test-section size. Then the time and mass scale factors might be adjusted so the model will operate at the full-scale Reynolds number. Usually, all dimensionless ratios cannot be maintained at full-scale values with reasonable choices of materials and scale factors in available test facilities. In such cases, compromises are made, based on experience and knowledge of the problem, by which the less important dimensionless ratios are allowed to deviate from full-scale values. If a proper choice is made, the resulting model will be classified as adequate; if a poor choice is made, the model will be distorted.

Scale Effects

Scale effects are often discussed as though some fundamental difference existed in the behavior of a prototype and its model. These so-called scale effects are actually measures of the distortion of the model, resulting from

unintentional or unavoidable failure to maintain full-scale values of significant dimensionless parameters. However, if very complex or partially understood phenomena are being investigated, it is advisable to evaluate this distortion by testing two models of different scales or one model and the prototype.

Launch-Vehicle Dynamic Models

It is well established that models can be used most effectively if they are individually designed to study specific problems. Table I gives some idea of the difficulty involved in scaling models for studying various launch-vehicle dynamic problems. The problem areas are shown on the left and the more important dimensionless ratios associated with each problem are listed on the right. A brief description of some of these problems will illustrate the scaling problems involved.

Vibrations.- Two kinds of beam-type vibrations are shown, one each for the lateral and longitudinal directions. Local vibrations are also listed in order to include shell and plate vibrations of local skin sections and panels. The first two, or beam-type, vibrations could probably be included in one model but are separated for clarity. If the vehicle being scaled behaves as a simple, or Euler, beam, the model must be scaled from the first two dimensionless ratios involving geometry, mass, Young's modulus, and frequency. However, if rotary inertia and shear effects are important, the model must be scaled as a Timoshenko beam and the additional ratios involving the shear modulus, effective shear area, and mass radius of gyration of the cross sections must be included. If local vibrations are the problem, still more dimensionless ratios must have equal values for model and prototype. Additional factors which appear are shell thickness, internal pressure, and density and depth of the liquid contained in the vehicle tanks. It is apparent that two models, one for beam-type vibrations and a second for a typical local section, would probably be a better approach than a single model scaled to duplicate both types of vibration.

Slosh.- Another problem being studied extensively with models is that of sloshing liquids. As described in reference 11, three dimensionless ratios must be satisfied if the container is rigid. Two of these ratios can be identified as the Reynolds and Froude numbers. The important quantities are geometry; liquid depth, density, and viscosity; and acceleration. Since all model tests are usually performed in a 1g acceleration field, it is difficult to meet the requirements for true similitude. However, by choosing fluids for the model which give a reasonable compromise for scaled density and viscosity, adequate models have been developed. If the container is not rigid, but elastic, several additional dimensionless ratios must be satisfied by the scaling (ref. 12). These ratios turn out to be essentially the same as those for local vibration but the reference proposes techniques for building adequate models for the phenomena. Still another possibility for slosh coupling occurs when the fluid container is part of an elastic vehicle. In this case, the lateral vibration parameters must be scaled as well as the sloshing parameters.

Buffeting.- Dimensionless ratios which are known to require scaling in modeling for aerodynamic buffeting are Mach number and Reynolds number (ref. 13). Careful attention must be given to geometry and local configuration details

since the scale of roughness, ϵ, is also expected to influence the results. A dimensional analysis of all pertinent quantities is contained in reference 14. As presented in table I, the ratios apply only for buffet on a rigid vehicle. If the responses of the vehicle must be determined in addition to pressure fluctuations, the buffet model may be required to scale the lateral vibration characteristics of the vehicle (for gross buffet) or the local vibration characteristics (for local buffet).

Flutter.- Flutter models have been used for many years in aircraft development and this experience applies directly to launch-vehicle flutter. New scaling, construction, and testing problems will be those normally associated with new configurations. An excellent discussion of flutter modeling techniques is given in reference 6.

Ground winds.- The last problem to be mentioned is ground winds. A satisfactory analytical treatment of this problem is still unavailable so models are being used almost exclusively in design. Local geometry and roughness have been shown to be very important parameters (ref. 14). The major aerodynamic parameter is Reynolds number. Additionally, lateral vibration properties must be scaled in order to study the response. Mach number, usually important only in the sense that it must be much less than one, is anticipated to cause difficulty in scaling future very large vehicles, such as Nova. For these very large vehicles, available wind tunnels limit the size of the model with the result that velocity must be increased to obtain full-scale Reynolds number. For a vehicle the size of Nova, model velocity must be increased to the point where Mach number becomes significant and model results might be distorted.

APPLICATIONS TO LAUNCH VEHICLES

One-Fifth-Scale Vibration Model of Saturn

The complexity of launch-vehicle structures has increased until analytical techniques for predicting their vibration characteristics, for use in stability and dynamic loads studies, are not always reliable. Therefore, a 1/5-scale dynamic replica model of the Saturn SA-1 launch vehicle was constructed at Langley Research Center to establish the feasibility of obtaining required experimental vibration data with a model. Model and full-scale vibration test vehicles are shown in their vibration towers in figure 2. The model is 32 feet high (compared with 160 feet for the full scale) and weighs about 7,500 pounds (compared with 935,000 pounds for the full scale).

Description.- The 1/5-scale Saturn model was built for the study of lateral bending vibrations; therefore, the important parameters to be scaled were the mass-stiffness ratios. Such things as aerodynamic fairing and fuel piping were not scaled since they did not contribute to stiffness; however, lead ballast weights were used to simulate their mass. Furthermore, the vibrations of principal interest were the overall vehicle modes, so local panel stiffnesses were not scaled. Such things as fuel sloshing and the suspension system were considered to have a secondary effect on the overall vehicle vibration and so were not scaled for the initial part of the test.

The type of scaling chosen for the Saturn model was a component-by-component uniform reduction of dimensions to one-fifth of the full-scale values, using the same materials as the full scale. This replica type of scaling was chosen because of the structural complexity of the Saturn booster with the resulting difficulty of determining accurate equivalent stiffness and mass properties for the many multiple-beam trusswork assemblies incorporated in the vehicle. An example of model duplication of full-scale multiple-beam structure is shown in figure 3. This figure is a close-up view of the base of the vehicle and shows that structural details such as skin corrugations, built-up riveted beams, tension rods, and longitudinal stiffeners in the outer tanks have been duplicated on the model; however, details such as the number of rivets, aerodynamic fairing supports, and piping supports are not true scale reproductions.

Two important structural simplifications were made on the model. First, the engines were simplified as shown in figure 4. Only the total weight, center of gravity, and moment of inertia were scaled. The simulated engines were firmly attached at the gimbal point without attempting to scale actuator stiffnesses. Second, some ring frames were omitted from the shell structure of the second stage. A view of the aft end of the second stage showing its internal construction is shown in figure 5. About 70 percent of the second-stage weight is contained in the ballast tank at the center, which is supported by the eight radial trusses attached to the outer shell. The outer shell is attached to the first stage only at the eight points at the ends of the radial trusses and thus forms the principal load structure of the second stage. Several ring frames on the full-scale vehicle were omitted from the outer-shell load-carrying structure on the model, resulting in some distorted vibration results which will be discussed subsequently.

Scaling.- The Saturn model was scaled by selecting a length scale factor L_m/L_p of 1/5 and using the same materials on the model as on the prototype. Therefore, the following relations are established:

$$\frac{E_m}{E_p} = \frac{\rho_m}{\rho_p} = \frac{\nu_m}{\nu_p} = 1$$

Then, in order to maintain the dimensionless ratios of table I for lateral vibrations, the mass and time scale factors must be:

$$\frac{M_m}{M_p} = \frac{1}{(5)^3}$$

$$\frac{\tau_m}{\tau_p} = \frac{1}{5}$$

Other relationships between model and prototype parameters, resulting from the dimensionless ratios, are:

1. Mass moment of inertia: $\frac{I'_m}{I'_p} = \frac{1}{(5)^5}$

2. Bending stiffness: $\frac{(EI)_m}{(EI)_p} = \frac{1}{(5)^4}$

3. Bending frequency: $\frac{f_m}{f_p} = 5$

4. Sloshing frequency: $\frac{f_m}{f_p} = \sqrt{5}$

5. Shell frequency: $\frac{f_m}{f_p} = 5$

Comparison of the bending and sloshing frequency ratios shows that the full-scale bending-sloshing frequency relationship is not maintained on the model. Thus, the interaction of vehicle bending with sloshing on the model will not represent directly the full-scale situation. For the Saturn configuration, where the first sloshing frequency is lower than the first bending frequency, the reduction to model size separates the frequencies, thus tending to uncouple the sloshing from the bending modes. The shell frequency relationship is based on an unstiffened shell with the same material and internal pressure in both model and full scale. Comparison of the bending with the shell frequency ratio shows that interaction of local shell vibration with vehicle bending vibration should be the same on the model as on the full scale in those cases where model construction and internal pressure are the same as the full scale.

Results.- Some results of the model vibration test are shown in figures 6, 7, 8, and 9. In figure 6 the first vibration mode of the model and full-scale vehicles is shown with the vehicle ballasted to simulate the maximum-dynamic-pressure weight condition. This figure shows almost exact agreement between model resonant frequency, when adjusted by the scale factor, and the full-scale resonant frequency. In order to obtain such good agreement, it was necessary to duplicate, on the model, the suspension system used to simulate free-free boundary conditions on the full-scale vehicle. The mode shapes of the full-scale and model vehicles are in good agreement as can be seen from comparison of the circles with the square symbols. The booster outer tanks, which are free to deflect independently of the center tank except at their ends, are shown in this figure to have the same deflection as the center tank, and this mode has the appearance of the more conventional bending modes obtained with nonclustered vehicles.

In contrast, the second vibration mode, shown in figure 7, shows one of the unusual vibration modes associated with the clustered arrangement of the Saturn booster. There is about a 10-percent difference in frequency between model and

full scale in this mode, and comparison of the circles with the squares shows fairly good agreement of model with full-scale mode shape. The typical outer tank indicated by the flagged symbols is seen to deflect in the opposite direction as the center tank. Cross-section A-A at the midsection of the booster shows that when the center tank deflects upward as indicated by the arrow the outer tanks are deflecting independently in the downward direction. This unusual mode shape where the outer tanks deflect in the opposite direction from the center tank is associated with the clustered arrangement of the booster tanks and has been termed a cluster mode.

The effect of omission of the ring stiffeners from the outer shell of the second stage is illustrated by figure 8, which shows the fourth vibration mode of the 1/5-scale Saturn model. In the area of the second stage two deflection curves are shown. The open circles indicate the deflection of the outer shell and the solid circles the deflection of the inner ballast tank. The data indicate that the outer shell and the ballast tank are deflecting in opposite directions. This can be explained by examination of cross-section B-B. The solid lines in this sketch indicate the undisturbed position of the water-filled ballast tank, the eight radial trusses, and the outer shell; the data points indicate the experimentally determined vibration amplitude. This cross section shows that the outer shell is vibrating in a shell mode with seven waves, while the center tank is translating. The deflections measured at points A and B on the inner and outer tanks, respectively, are in opposite directions, as shown also in the sketch in the center. The shell mode in the second-stage outer shell shown here was observed on the model in the higher-frequency modes for most weight conditions; however, no shell modes in the second stage were observed on the full-scale Saturn vibration test vehicle.

The mode shapes and resonant frequencies which have been shown were measured at the weight condition which simulates flight near maximum dynamic pressure. An indication of how the resonant frequencies of model and full scale compare at other weight conditions is shown in figure 9. The ordinate is full-scale frequency, in cycles per second, and the abscissa is water level in the booster stage, in percent. Zero percent corresponds to first-stage burnout while 100 percent corresponds to lift-off. The previously shown data were measured at 48 percent full. Model frequencies, adjusted by the scale factor, are shown as circles while full-scale frequencies are shown as squares. The first bending mode frequency shows almost exact agreement except at lift-off, where the model frequency is about 7 percent high. The first cluster mode frequency is predicted by the model to within 10 percent. For higher modes, agreement between model and full scale is not as good.

The data presented in figure 9 were obtained using an eight-cable suspension system which duplicated a similar suspension system used for full-scale tests. Earlier model tests, using a two-cable free-free suspension system which gave much better separation between suspension frequency and bending frequency than the eight-cable system had given model first bending frequencies 5 to 10 percent lower than full-scale frequencies. This result indicated the importance of properly accounting for suspension system effects in comparing model and full-scale data and of properly interpreting ground test data when extrapolating to flight conditions.

Saturn V Dynamic Models

Figure 10 illustrates the present modeling project, which is a 1/10-scale replica model of the Saturn V. The model is 36 feet high, including the Apollo payload. The general type of construction of the full scale is shown including skin stringer, waffle pattern, integrally milled stringer, and corrugated skin. The model will duplicate all of these essential details up to the Apollo payload. For the Apollo payload, simulation techniques are being used, whereby the EI, AE, GJ, and mass distribution are matched.

On the right of the figure is shown a scalloped or multicelled tank concept, which is also being constructed and will replace the cylindrical first stage for later tests.

In addition to the 1/10-scale model, a 1/40-scale model is being constructed which is shown in figure 11. An illustration of the details of the model construction is shown in figure 12. On the lower left is shown the five-engine simulation. Next to the engine are two fuel slosh simulators, using a "bird-cage" spring-mass assembly. These simulators can be placed at various positions on the vehicle, and the spring constants as well as the mass can be changed.

Fuel Slosh

One of the problem areas in testing liquid-fueled vehicles is the effect of fuel slosh. In figure 13 several significant frequencies are plotted against flight time for the cylindrical tank as well as the scalloped tank. First bending is shown as a dashed line, flight fuel slosh as a solid line, range of pitch frequency by the shaded area, a line depicting a 1/10-scale model fuel slosh frequency and full-scale ground-test frequencies. A rather large separation in frequency exists between the fuel bending mode and the flight fuel slosh frequency. Thus coupling of the fuel slosh mode with the elastic mode will be rather weak even in the flight case. A 1/10-scale model would have lower frequencies as indicated, but since the fuel slosh is already rather well uncoupled, the 1/10-scale model results should duplicate the full-scale flight results with very minor differences. As a matter of fact, even for full-scale ground tests, the proper fuel slosh frequency would not be exactly simulated as shown due to the 1g field in which the vehicle must be tested.

On the right side is shown the effect of the system frequencies of a scalloped tank. Note that the bending frequency has been reduced. This is due to the basic design criteria of maintaining the same internal pressure and vertical load-carrying ability as in the cylindrical tank. This results in more material being used closer to the tank center thus reducing the moment of inertia and consequently the bending stiffness. On the other hand, the fuel slosh frequency has increased due to compartmentation. Thus, the two frequencies are approaching each other while moving the fuel slosh frequency away from the rigid-body frequency, which, of course, is beneficial. However, a definite coupling between fuel slosh and the fundamental vibration modes now exists. In cases such as this, the adequacy of the structural duplication of the model may be checked against analytical representation for fuel slosh frequencies well removed from the coupling possibility. Then with confidence in the structural

adequacy, the effect of fuel slosh having frequencies in the neighborhood of the fundamental frequencies may be estimated for control system design.

Buffeting

Buffeting forces on a launch vehicle arise as a result of unsteady flow around corners, bluff bodies, protuberances, etc., during transonic flight. Calculation of these oscillating pressures is virtually impossible, and resort to modeling techniques is necessary.

Several avenues are open to the modelist. One involves the detailed pressure measurement on a rigid scaled model, utilizing the pressures to calculate the vehicle response. A second method is to construct a flexible scaled model and to measure the desired output. Both methods are being used, each having its own advantages and disadvantages. The method to be discussed here involves the use of an elastic model in which the total vehicle response is measured. The pressure-measurement technique is described in more detail in reference 15.

It is convenient to separate buffet into two types, depending on the relation between the frequency of the input with respect to (1) the frequency of the vehicle lateral bending modes, and (2) the frequencies of the local structural elements. That is, if the major input frequency can excite the lower structural modes the term "gross buffet" will be used, whereas if the input frequency is relatively high and will excite local structures and panels, the term "local buffet" will be applied.

Gross buffet.- Modeling for gross buffet studies requires simulation of the aerodynamic shape, Mach number, Reynolds number, and proper scaling of the structural parameters to provide simulation of the lower lateral modes and frequencies. In order to explore the problems associated with structural and aerodynamic scaling of buffet, a 1/25-scale model of a typical launch vehicle was built and tested at Langley Research Center. Figure 13 shows the model. The geometrical scale of this model was established by the maximum size that could be accommodated in the tunnel without inducing severe blocking at transonic speeds.

One of the major difficulties in performing such a test is to reduce as much as possible the effect of the model restraining system since primary interest is centered on results applicable to the flight of the vehicle in a free-free condition. For aerodynamic reasons, no supporting structure should be exposed to the airstream, either ahead of or around the model. This dictates a so-called sting support which is essentially a cantilevered beam, illustrated in figure 14. The model is connected to this beam by flexible supports as shown. Thus there are introduced several additional elastic degrees of freedom which do not appear on the free-flight hardware. For the present model, the ratio of the sting support frequency to the model support frequency was made as low as possible in order to avoid large coupling effects with the lateral bending mode. The following table indicates the resultant frequencies:

Sting - model	12 cps
Model - pitch (rigid)	22 cps
First lateral bending	85 cps
Second lateral bending	223 cps

As can be seen, a reasonable separation of the frequencies was obtained. The model pitch spring was designed mainly from the standpoint of static aerodynamic axial and pitch loads.

Two nose cone configurations were investigated, one straight cone cylinder as illustrated, and the same model with a bulbar nose. Strain gages were installed for the purpose of measuring the dynamic bending-moment response. Figure 15 shows the power spectra of the bending moment for a given Mach number and Reynolds number. Note that the bulbar nose shape induces a much greater response than the cone cylinder. The two large peaks shown correspond to the first and second lateral modes and there is little effect of extraneous modes. The response at the lower frequency portion is due to the sting model restraint but it is felt that this will not influence the results at the lateral bending frequencies.

The results of this investigation indicate, in general, that useful information concerning gross buffet can be obtained using a small elastic model; and, specifically, that a bulbar nose induces more elastic buffet response of the model vehicle than a conical nose.

Local buffeting.- Local buffeting, as the name implies, involves only a small portion of the vehicle, i.e., panels, adapters, fairings, etc. The fundamental frequency of these components is usually much higher than the lateral bending modes and, hence, will not normally be coupled. However, there always remains the possibility of a lateral deflection inducing local buckling, which could have a large influence on the response to turbulence of a particular local section. To construct a complete model of the vehicle simulating the local stiffness is almost as large a job as building the prototype, particularly when an effort is made to simulate the panel edge conditions and structural damping. The model would, of necessity, be rather large and would be almost impossible to test in available transonic wind tunnels without flow blockage in the test section. An obvious solution is to utilize full-scale or large-scale components for tunnel tests. However, the proper turbulence environment would have to be artificially produced since the proper shape, protuberances, etc., are not in front of the test specimen. At the present time the only practical method is to measure the local pressures on a small, rigid model and attempt to estimate the effect of this pressure fluctuation on the local section by analytical means. A partial application of this technique to one configuration is presented in reference 16. Suffice it to say that techniques for studying local buffet are still in a developmental stage.

Ground Wind Model

A model of a launch vehicle for the investigation of ground wind loads will be discussed as a final example of the application of dynamic models. Ground winds are a problem because a launch vehicle is exposed to the variable surface winds during the final stages of the countdown when the gantry and protecting structure are removed. The loads induced on the launch vehicle by the winds may be divided into two components - a drag load parallel to the wind and a lateral load normal to the wind. The steady drag loads can be predicted adequately since aerodynamic characteristics can be measured or estimated rather well. However, the loads normal to the wind direction are oscillatory in nature due to a flow breakdown around the cylindrical vehicle and theoretical procedures, except for the Von Karman vortex shedding concept, are not available. Hence, model techniques are mandatory.

Both full-scale and dynamic model investigations of the ground wind loads on a Scout launch vehicle have been conducted by the Langley Research Center. The Scout is a four-stage solid-propellant booster which is capable of putting a 150-pound payload into a 300-nautical-mile orbit. Measurements of the bending moment were made on the prototype and on a 15-percent scaled model as shown in figure 16. Due to its proximity to the vehicle, the gantry tower was also scaled for the model tests. The model was tested in the Langley 16-Foot Transonic Dynamics Tunnel and the unpublished model results to be shown were obtained by Mr. Wilmer H. Reed, III. Full-scale test results are from reference 17. The principal nondimensional parameters used in model design were Reynolds number, reduced frequency $L\omega/V$, and mass ratio $m/\rho L^2$. The tunnel selected for the test can use either air or Freon 12 as a testing medium, but for this study Freon 12 was found to be desirable principally from the standpoint of Reynolds number simulation. The model was a steel shell with some aluminum used in upper-stage areas. It contained distributed mass ballasting in order to simulate the first bending frequency of the vehicle since the phenomenon of interest was the oscillatory response normal to the airstream.

Results of the investigation are shown in figure 17. The root-mean-square bending moment at the base of the vehicle is plotted against the average wind speed. The full-scale test results are indicated by the solid points and the model results by the open symbols. The model results have been corrected by the method of reference 18 to account for differences in frequency and damping between the model and full scale. The square points are results for a side wind, as illustrated at the top of the figure, the circular points are for the wind first passing through the tower, and the diamonds are for the wind passing first over the model, then over the tower. In each case, the bending-moment response is in a plane normal to the wind direction.

Considerable scatter is evident in the full-scale data, although the loads are higher than those predicted by the model. Insofar as design of the particular vehicle is concerned, the bending moments shown are well below ultimate bending moment and no operational problem is anticipated. However, from a modeling viewpoint, an explanation of the distortion between model and full scale is desirable. A possible explanation would be that natural turbulence in the atmosphere is causing larger response on the full-scale vehicle than the

low turbulence flow in the wind tunnel causes on the model. Note that model results are in much better agreement with full-scale data when the airflow is through the tower instead of from the side or front. Since flow through the tower would tend to equalize turbulence levels on the full scale and the model, this would tend to support the turbulence explanation for the distortion in the results.

Summarizing Statement

As mentioned previously, dynamic models were extensively used in support of the development of aircraft. Early in the development of large launch vehicles modeling techniques were not used due mainly to the crash programs under which they were conducted. With the advent of the large space program, however, reliability has become a key factor - in many cases only one or two expensive payloads of one kind are available and reliability has become vital. In order to improve reliability, dynamic models can play a paramount role, not only to obtain direct design data but also to check analytical techniques. So far, dynamic models have been used very successfully for vehicle vibration modes and frequency determination, fuel slosh studies, and buffeting and ground wind research. The model technique is advantageous from the standpoint of economy of money, men, and time.

Some of the remaining areas requiring further investigation and study are:

(1) Coupling of fuel slosh with flexible modes for the close coupling situation and development of better simulation techniques.

(2) Use of models to study the response of the shell-like structure to random disturbances such as buffeting and acoustics.

(3) Simulation of the proper aerodynamic input for ground wind models.

REFERENCES

1. Buckingham, E.: On Physically Similar Systems; Illustrations of the Use of Dimensional Equations. Physical Review, vol. 4, no. 4, 1914, pp. 345-376.

2. Olson, Harry F.: Dynamical Analogies. Van Nostrand Company, New York, N.Y., 1943.

3. Langhaar, Henry L.: Dimensional Analysis and Theory of Models. John Wiley & Sons, Inc., New York, N.Y., 1951.

4. Bridgman, P. W.: Dimensional Analysis. Yale University Press, New Haven, Conn., 1922.

5. Murphy, Glenn: Similitude in Engineering. Ronald Press, New York, N.Y., 1950.

6. Bisplinghoff, R. L., Ashley, H., and Halfman, R. L.: Aeroelasticity. Addison-Wesley, Cambridge, Mass., 1955.

7. Heldenfels, R. R.: Models and Analogs, for High-Temperature Effects in Aircraft Structure. Pergamon Press, New York, N.Y., 1959, pp. 323-354.

8. O'Sullivan, W. J., Jr.: Theory of Aircraft Structural Models Subjected to Aerodynamic Heating and External Loads. NACA TN 4115, 1957.

9. Brooks, G. W.: The Application of Models to Helicopter Vibration and Flutter Research. Pres. to 9th Annual Forum of the AHS, Washington, D.C., June 14, 1953.

10. Duberg, J. E.: Aircraft Structures Research at Elevated Temperatures. Pres. to Structures and Materials Panel of AGARD, September 1955.

11. Abramson, H. N., and Ransleben, G. E., Jr.: Simulation of Fuel Sloshing Characteristics in Missile Tanks by Use of Small Models. Southwest Research Institute, TR No. 7, April 1960.

12. Sandorff, P. E.: Principles of Design of Dynamically Similar Models for Large Propellant Tanks. NASA TN D-99, 1960.

13. Liepmann, H. W.: Parameters for Use in Buffeting Flight Tests. Douglas Report SM-14631, 1953.

14. Buell, Donald A., and Kenyon, George C.: The Wind-Induced Loads on a Dynamically Scaled Model of a Large Missile in Launching Position. NASA TM X-109, 1959.

15. Ezra, A. A., and Peterson, H. C.: Determination of Design Criteria for Transonic Buffeting Forces Acting on Launch Vehicles. ARS Preprint No. 2407-62, April 1962.

16. Rainey, A. G., and Runyan, H. L.: Structural Dynamics Aspects of the Manned Lunar Space Vehicle Launch Phase. SAE Preprint No. 513C, April 1962.

17. Jones, George W., Jr., and Gilman, Jean, Jr.: Measured Response to Wind-Induced Dynamic Loads of a Full-Scale Scout Vehicle Mounted Vertically on a Launching Tower. NASA TN D-757, 1961.

18. Thomson, W. T., and Barton, M. V.: The Response of Mechanical Systems to Random Excitation. Jour. Appl. Mech., vol. 24, no. 2, June 1957, pp. 248-251.

TABLE I

SOME STRUCTURAL DYNAMICS MODELING PARAMETERS

Problem area	Dimensionless ratios
Lateral vibrations	$\frac{m\omega^2}{E}$, $\frac{I}{L^4}$, $\frac{I}{KAL^2}$, $\frac{G}{E}$, $\frac{k}{L}$
Longitudinal vibrations	$\frac{m\omega^2}{E}$, $\frac{A}{L^2}$
Local vibrations	$\frac{\rho_w \omega^2 L^2}{E}$, $\frac{t}{r}$, $\frac{h}{r}$, $\frac{r}{L}$, $\frac{G}{E}$, $\frac{p}{E}$, $\frac{\rho_l}{\rho_w}$
Sloshing (rigid tank)	$\frac{\rho r^2}{\mu\tau}$, $\frac{h}{r}$, $\frac{a\tau^2}{r}$
Buffet (rigid vehicle)	$\frac{L\omega}{V}$, $\frac{r}{L}$, $\frac{\epsilon}{r}$, $\frac{p}{\rho V^2}$, N_M, N_R
Flutter	$\frac{L\omega}{V}$, $\frac{m}{\rho L^2}$, $\frac{S\alpha}{mL}$, $\frac{I\alpha}{mL^2}$, $\frac{\omega}{\omega_\alpha}$, $\frac{\omega_h}{\omega_\alpha}$, $\frac{x_o}{L}$, N_M
Ground winds	$\frac{L\omega}{V}$, $\frac{r}{L}$, $\frac{\epsilon}{r}$, $\frac{m}{\rho L^2}$, $\frac{m\omega^2}{E}$, $\frac{I}{L^4}$, $\omega\tau$, N_R

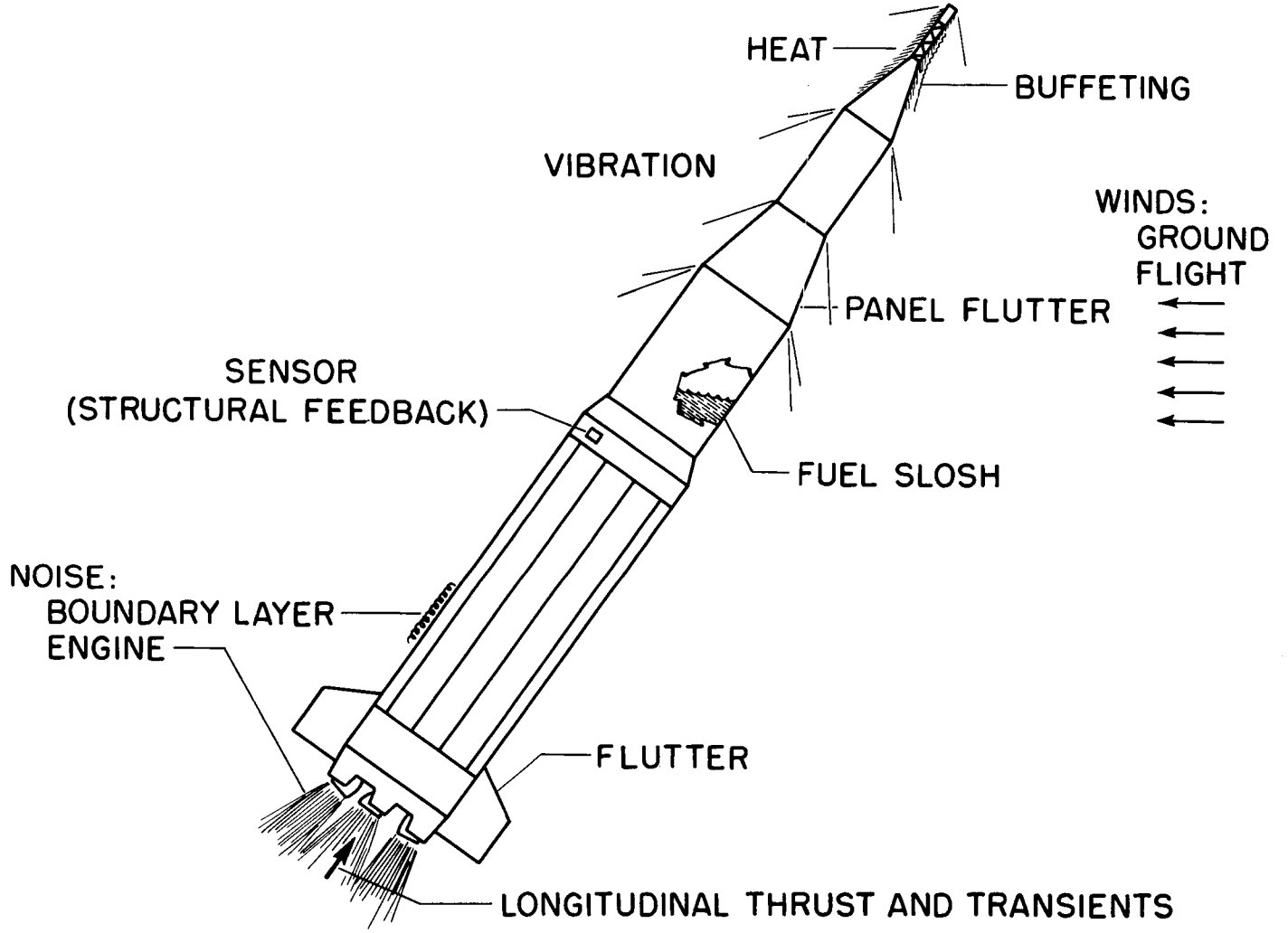

NASA

Figure 1.- Launch-vehicle problem areas.

	MODEL	FULL SCALE
LENGTH, FT	32	160
BOOSTER DIAMETER, FT	4	20
LIFTOFF WEIGHT, LB	7500	935,000

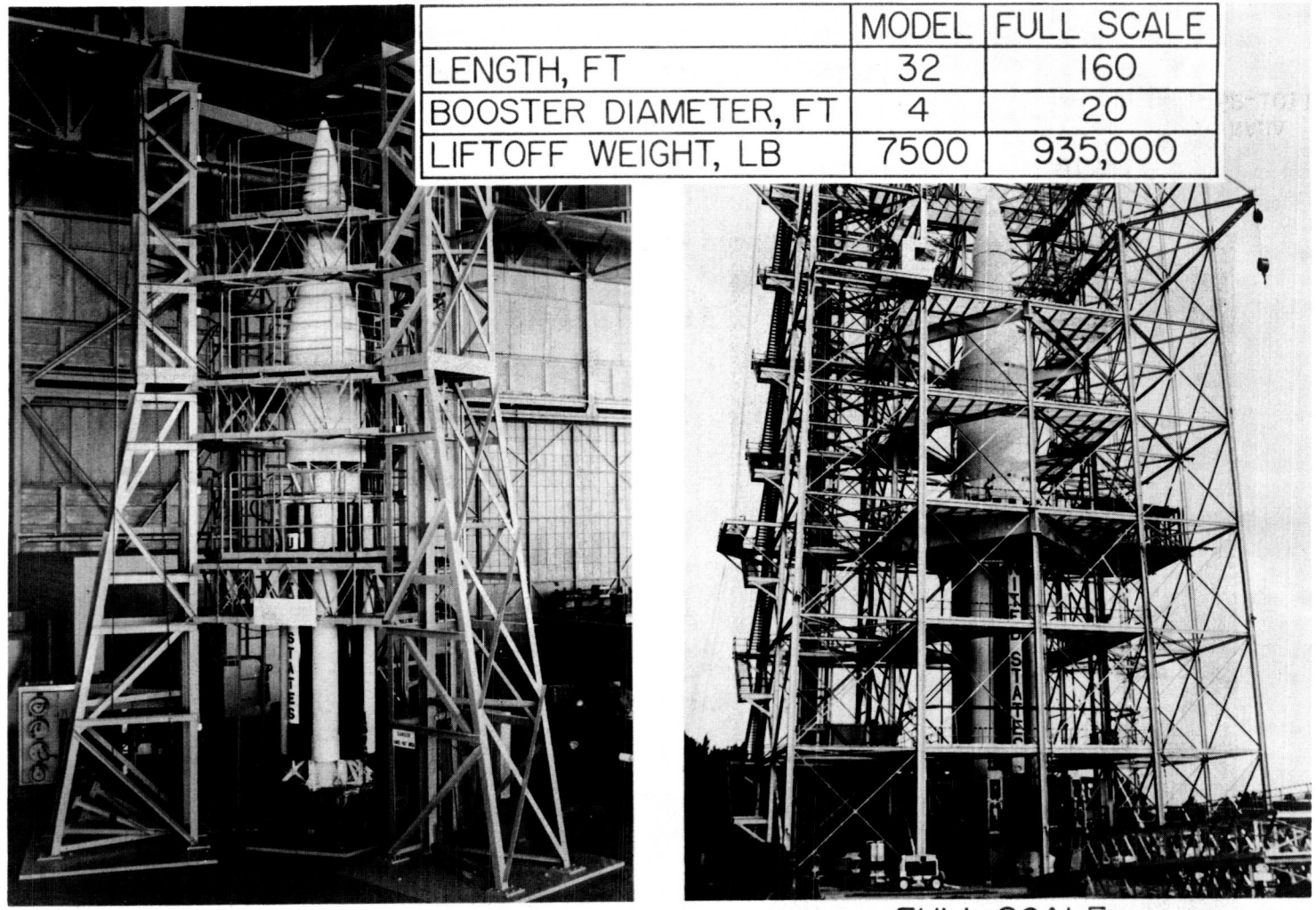

NASA
L-62-1012.1

Figure 2.- Model and full-scale Saturn vibration test vehicles.

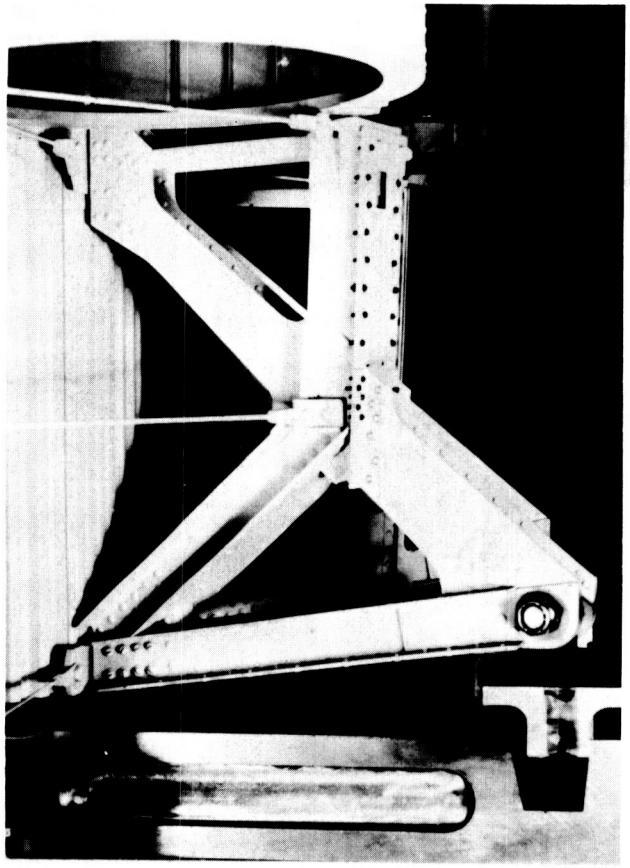

MODEL

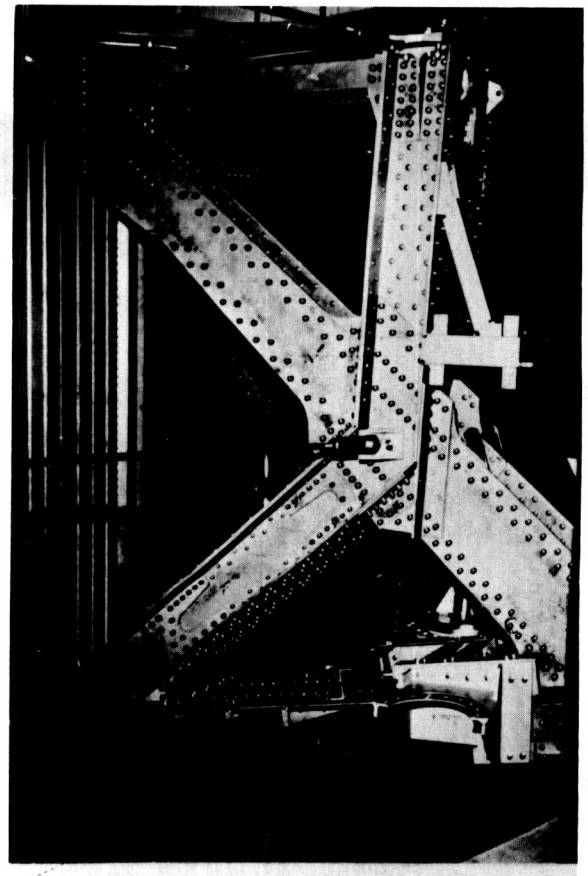

FULL SCALE

NASA
L-62-1011.1

Figure 3.- Saturn structural details.

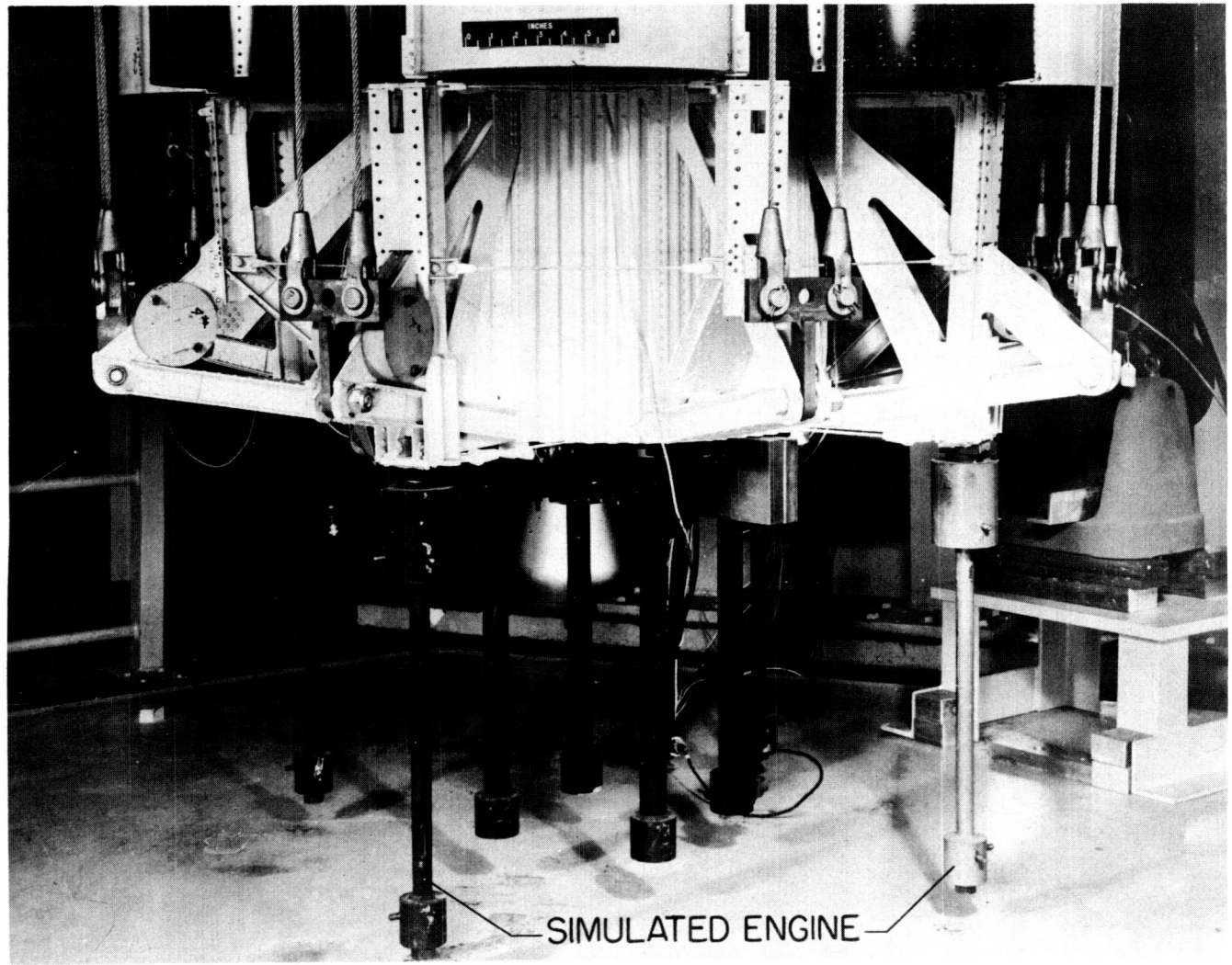

NASA
L-62-5095.1

Figure 4.- Photograph showing 1/5-scale Saturn engines.

NASA
L-61-2988.1

Figure 5.- End view of 1/5-scale Saturn second stage.

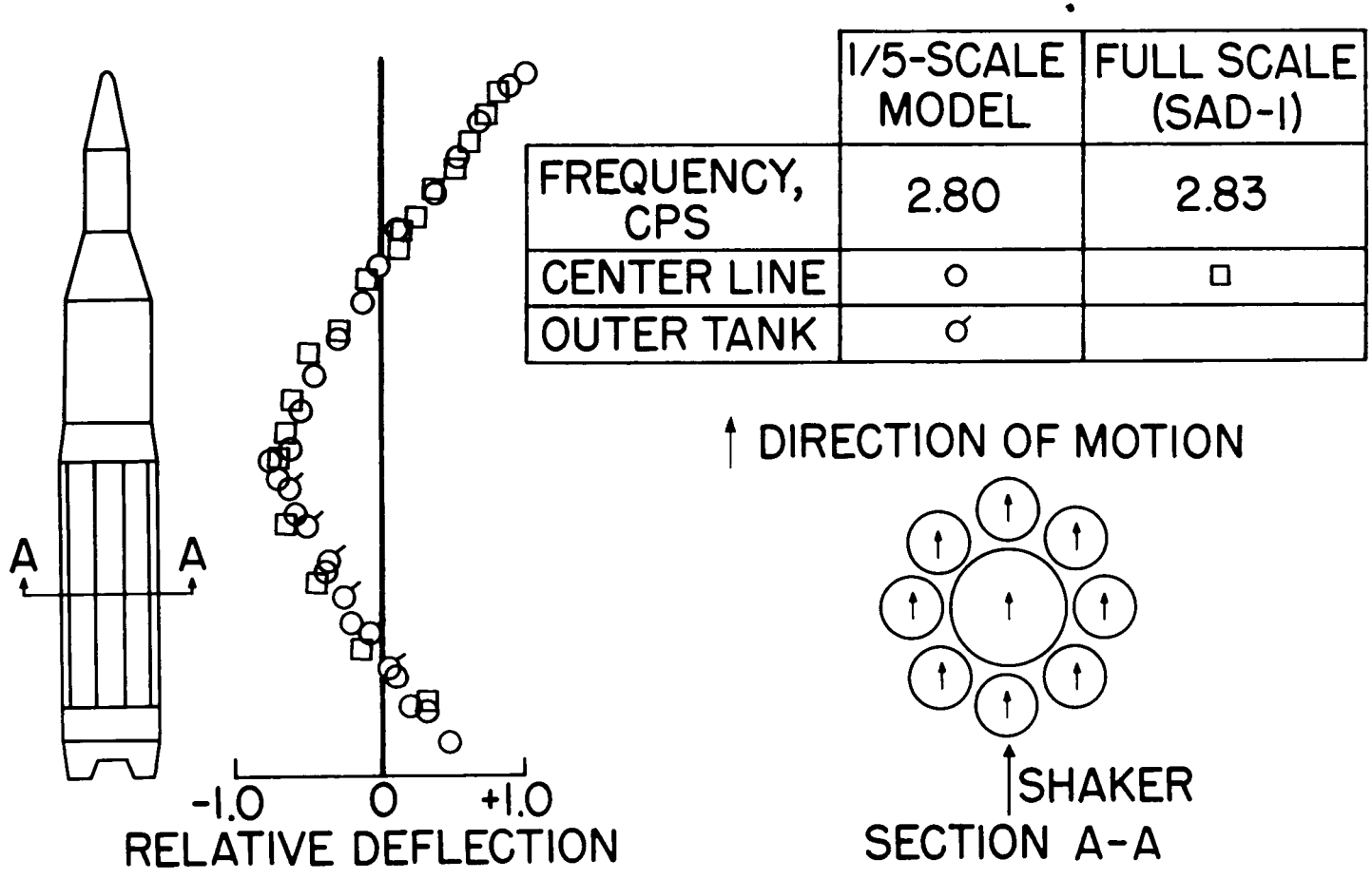

Figure 6.- First bending mode of Saturn, maximum dynamic pressure weight.

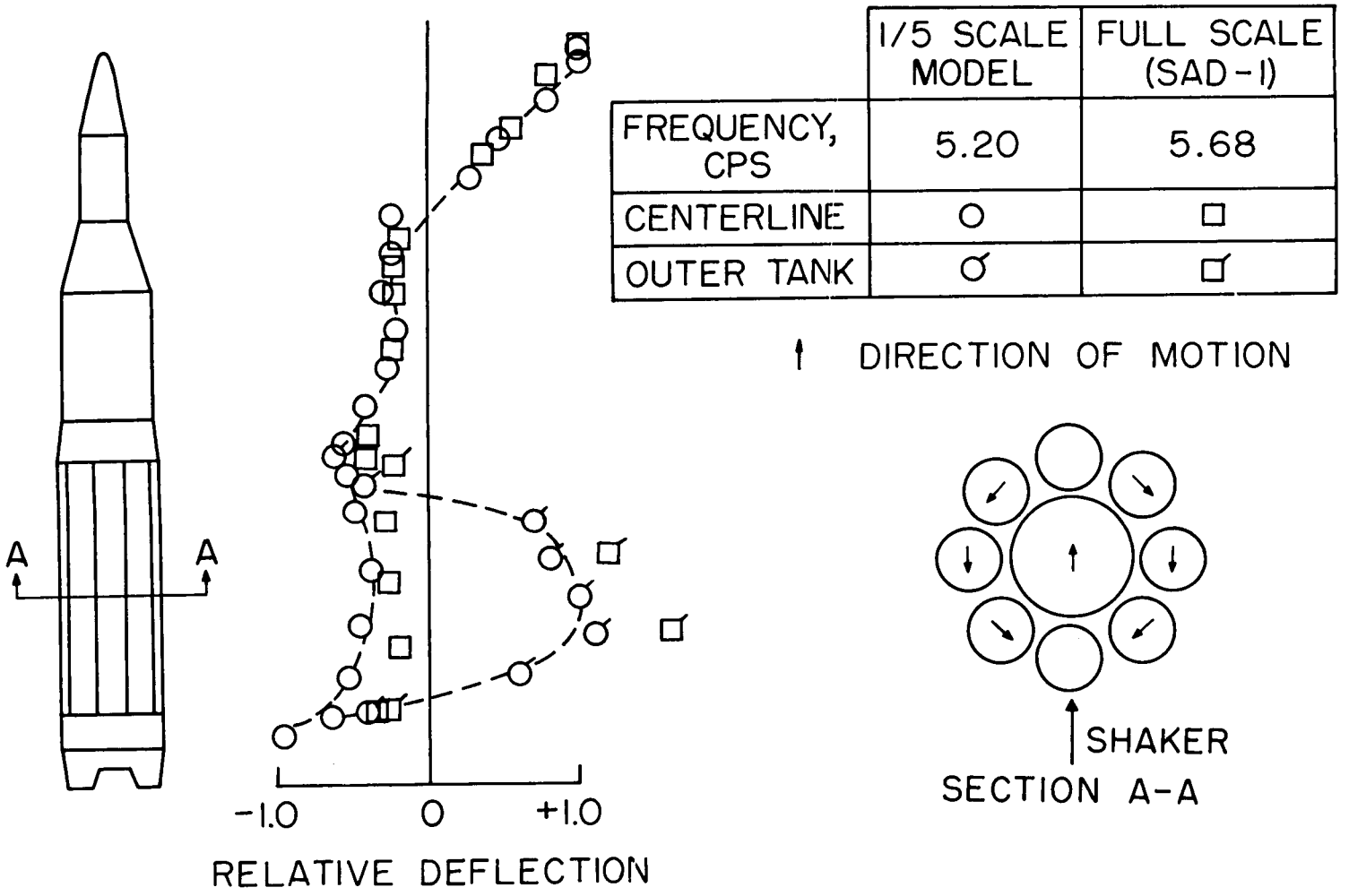

NASA

Figure 7.- First cluster mode of Saturn, maximum dynamic pressure weight.

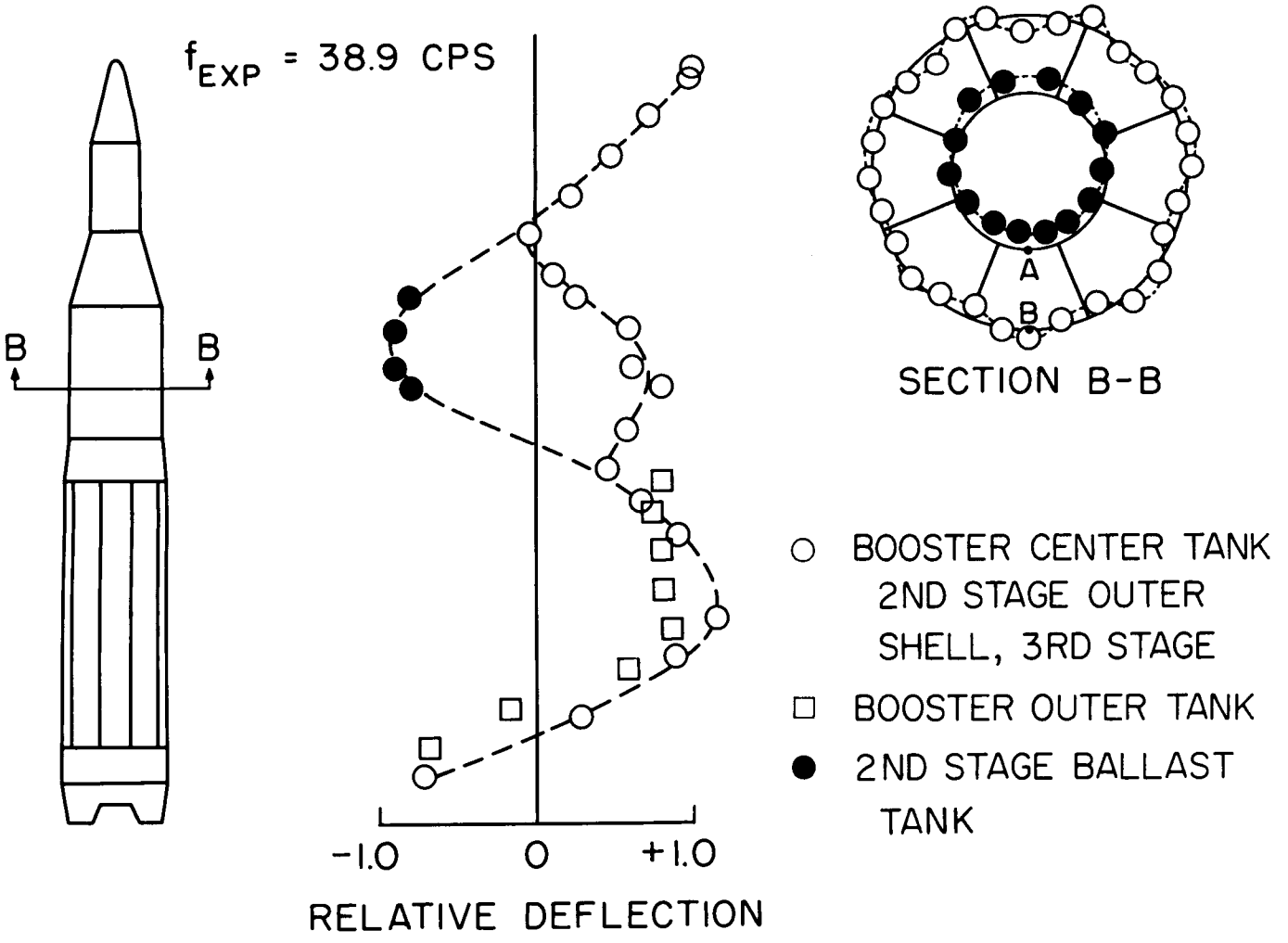

Figure 8.- Fourth vibration mode of 1/5-scale Saturn.

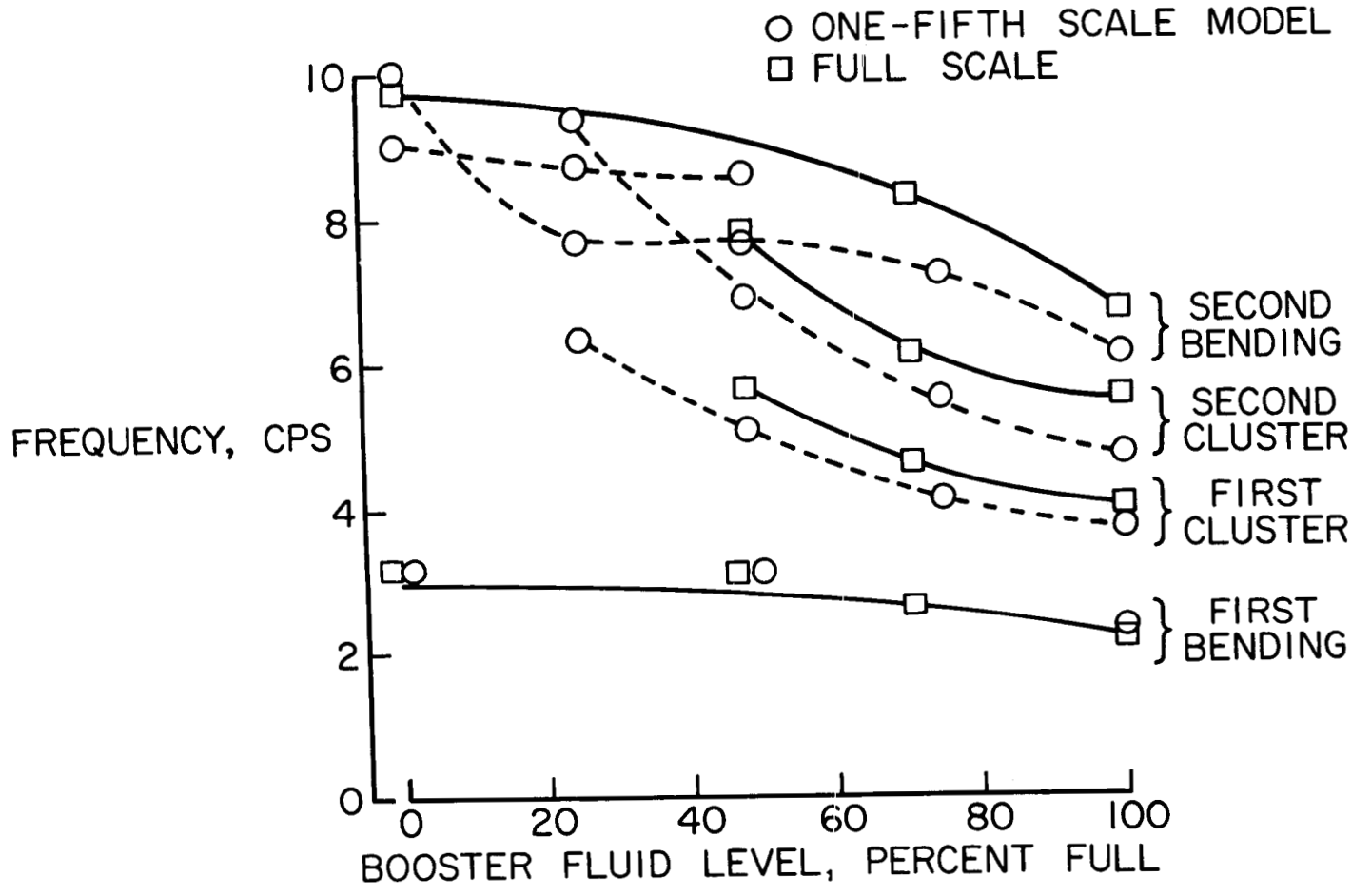

NASA

Figure 9.- Fundamental vibration frequencies of Saturn I.

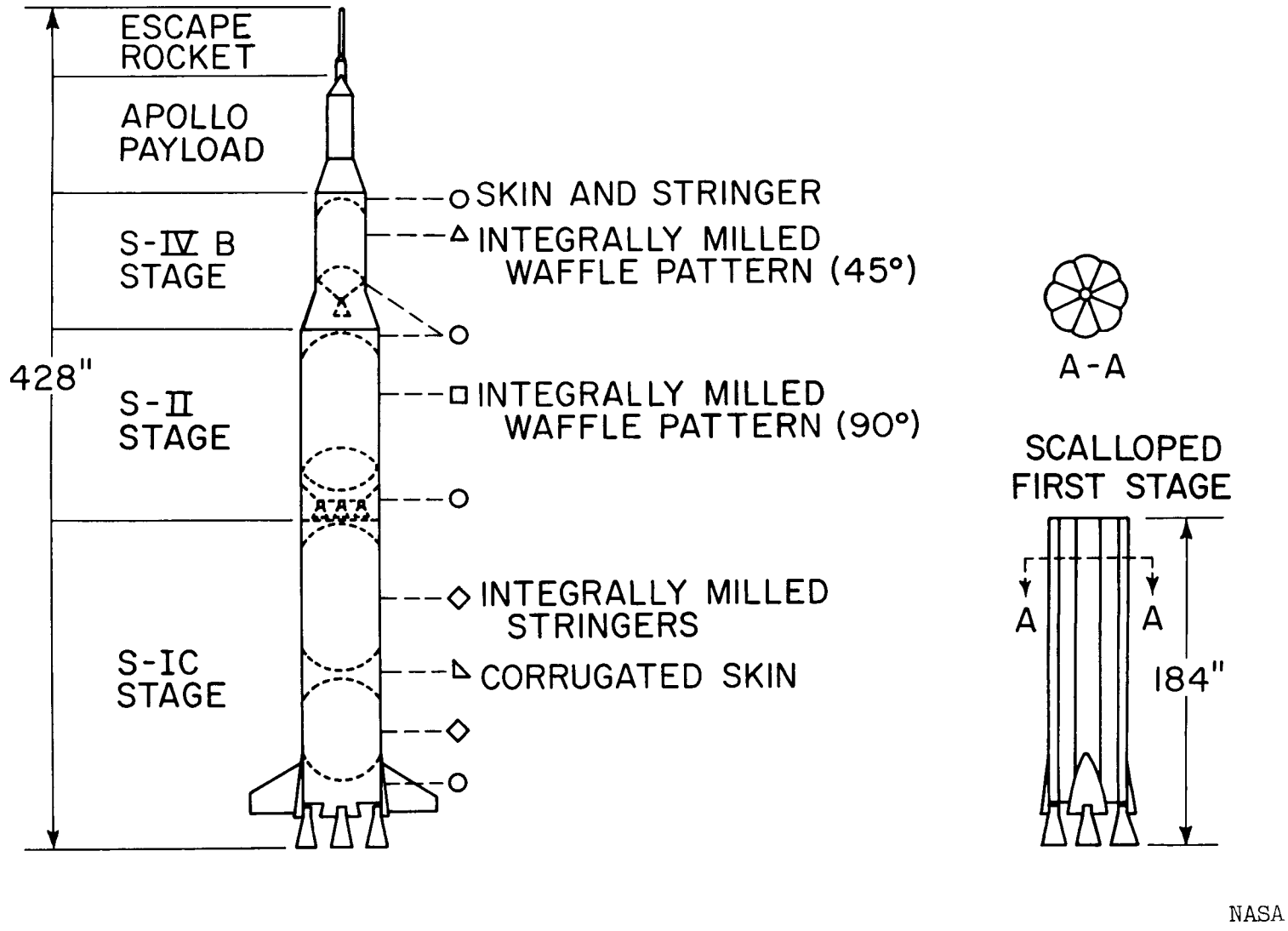

Figure 10.- One-tenth-scale model of Saturn V and scalloped first stage.

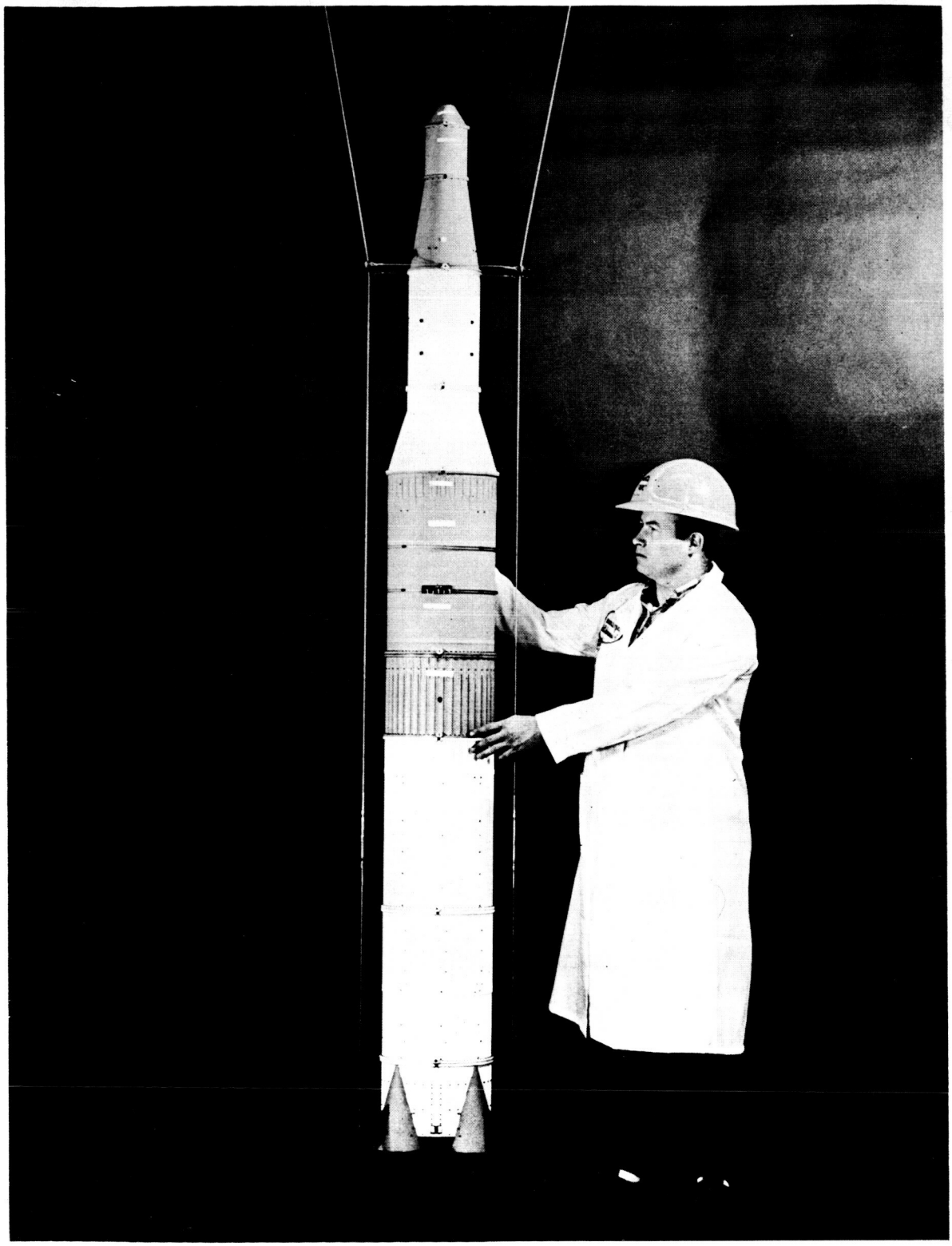

NASA

Figure 11.- Photograph of 1/40-scale model of Saturn V.

NASA

Figure 12.- 1/40-scale model details of Saturn V.

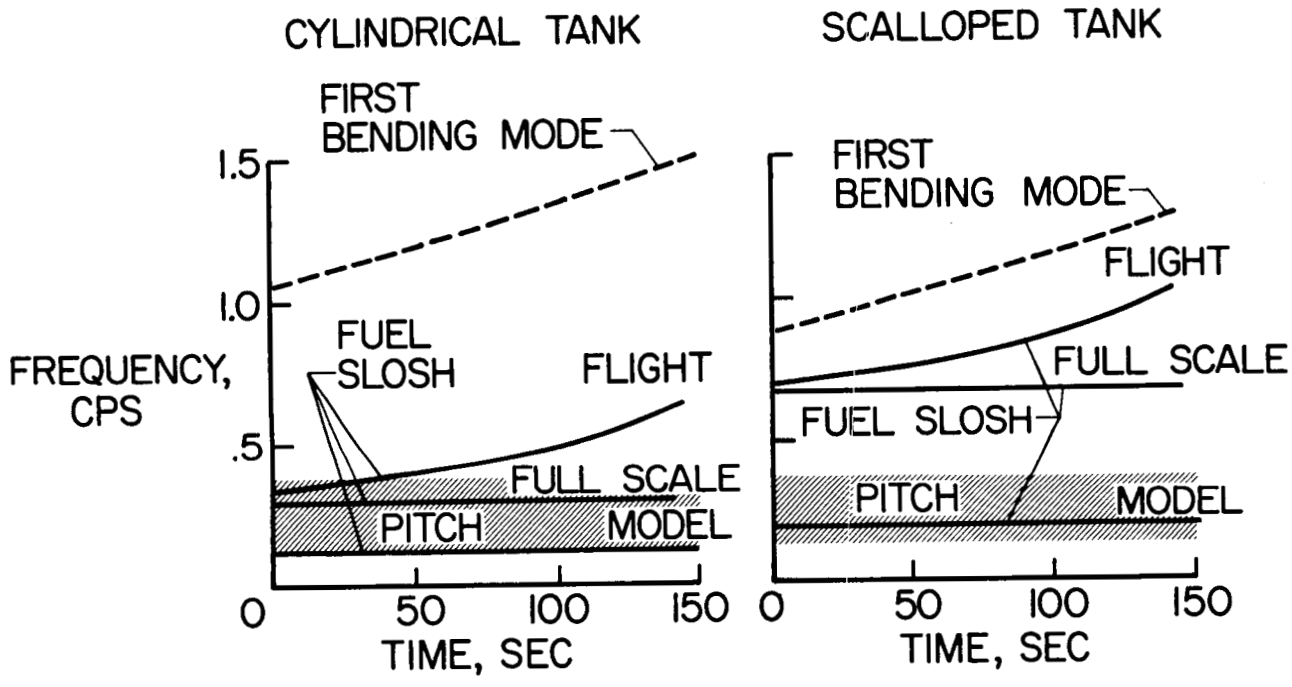

NASA

Figure 13.- Fundamental frequencies calculated for large launch vehicle for cylindrical and scalloped first stage.

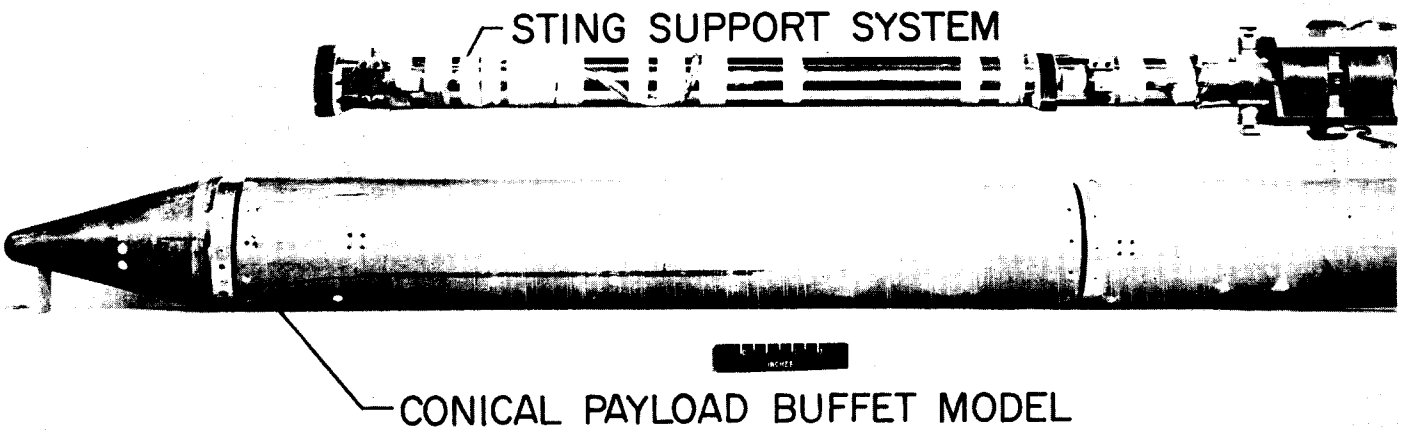

NASA
L-61-1191.1

Figure 14.- Photograph of buffet model and mounting sting.

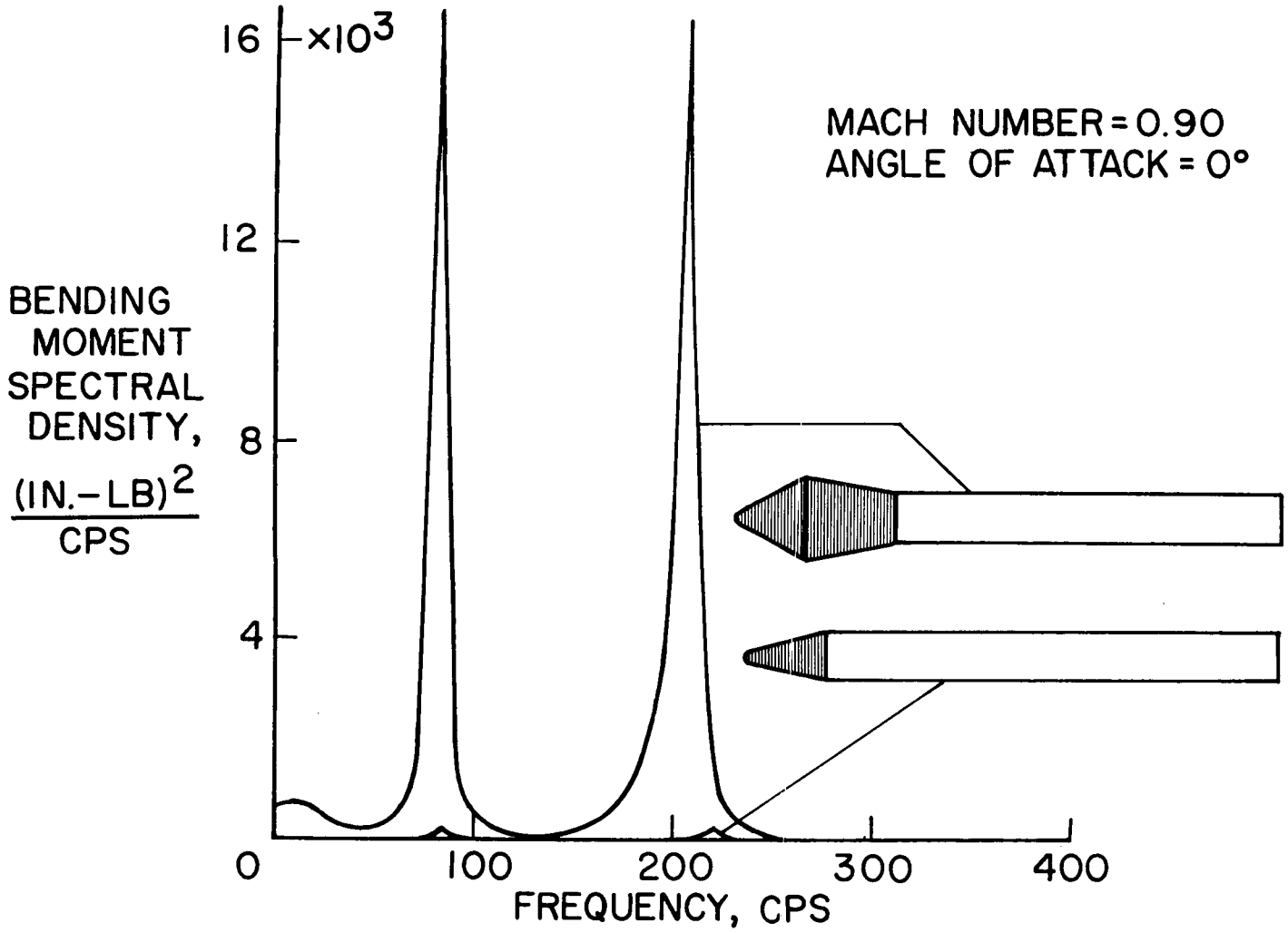

NASA

Figure 15.- Spectrum of bending-moment response due to buffet.

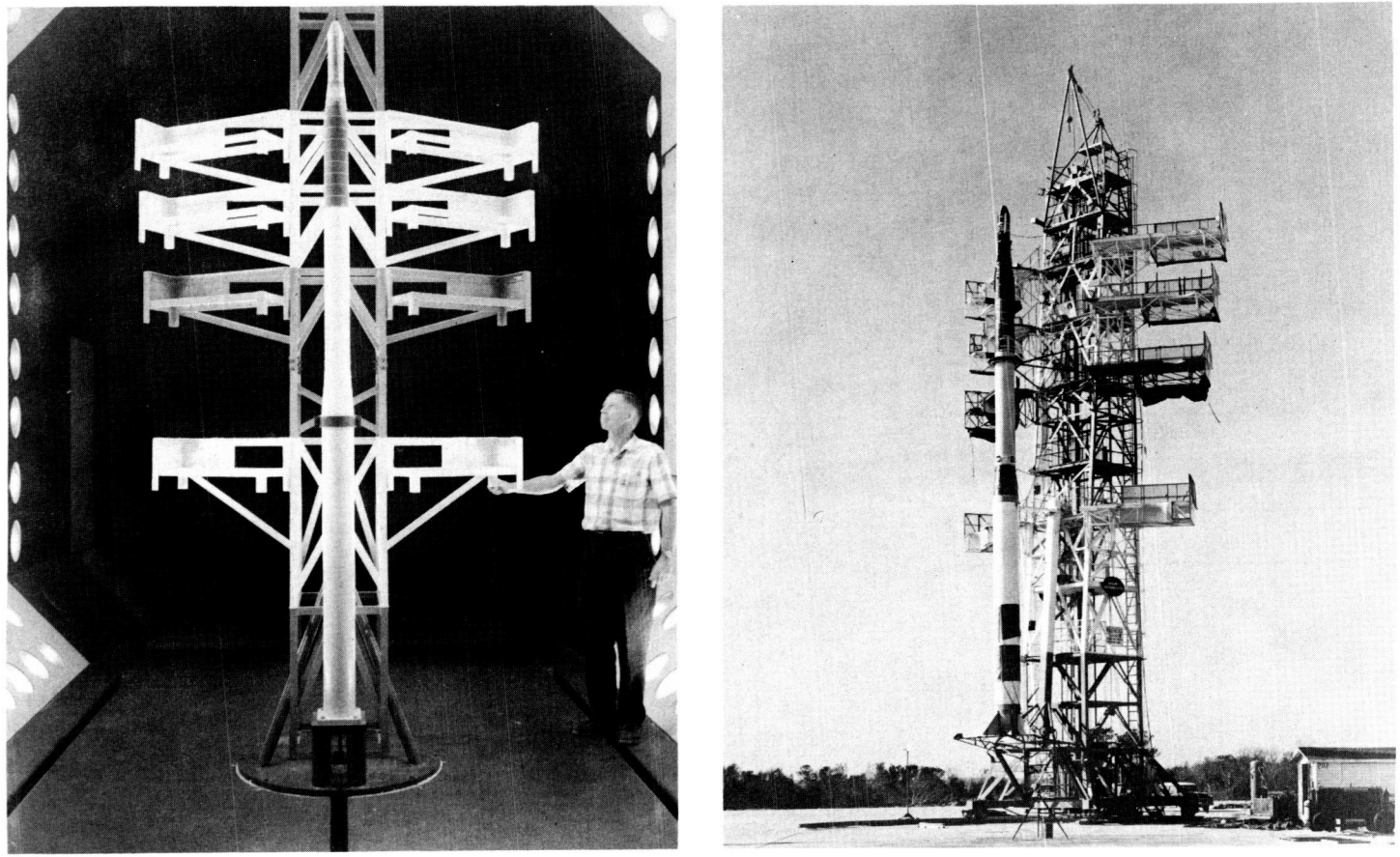

15-percent model. Full scale. NASA L-62-1018

Figure 16.- Model and full-scale Scout vehicles on launcher.

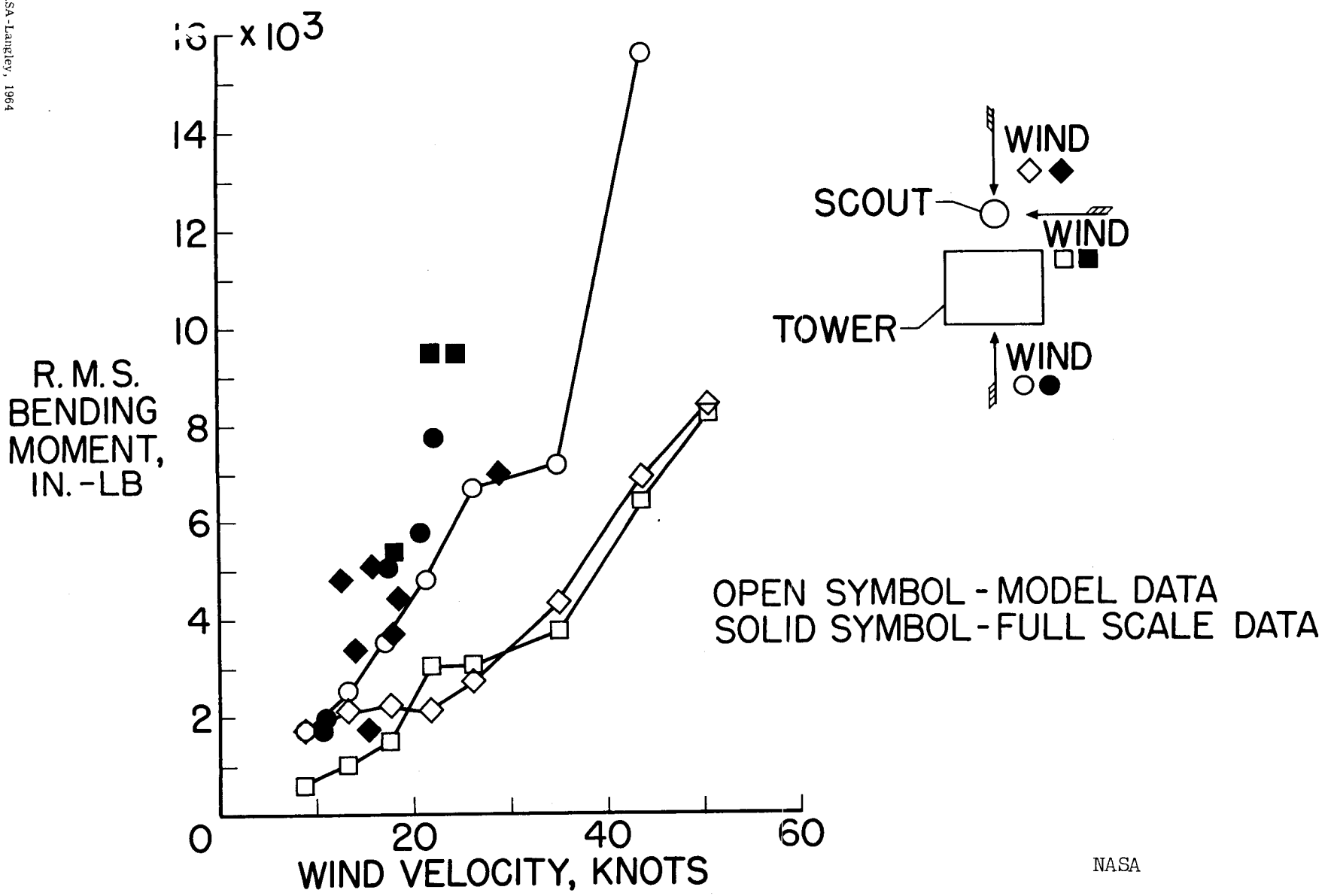

Figure 17.- Model and full-scale response of Scout to ground winds.

Table I. Johnson's data on solar spectral radiant flux (denoted by P_λ) for air mass zero
λ in microns; P_λ in watts $cm^{-2}\ \mu^{-1}$. Third column is the cumulative percentage of energy.

λ (μ)	P_λ (w/cm²μ)	cum. (%)	λ (μ)	P_λ (w/cm²μ)	cum. (%)	λ (μ)	P_λ (w/cm²μ)	cum. (%)	λ (μ)	P_λ (w/cm²μ)	cum. (%)
0.22	0.0030	0.02	0.395	0.120	3.54	0.57	0.187	33.2	1.9	0.01274	93.6
0.225	0.0042	0.03	0.40	0.154	9.03	0.575	0.187	33.9	2.0	0.01079	93.87
0.23	0.0052	0.05	0.405	0.188	9.65	0.58	0.187	34.5	2.1	0.00917	94.58
0.235	0.0054	0.07	0.41	0.194	10.3	0.585	0.185	35.2	2.2	0.00785	95.20
0.24	0.0058	0.09	0.415	0.192	11.0	0.59	0.184	35.9	2.3	0.00676	95.71
0.245	0.0064	0.11	0.42	0.192	11.7	0.595	0.183	36.5	2.4	0.00585	96.18
0.25	0.0064	0.13	0.425	0.189	12.4	0.60	0.181	37.2	2.5	0.00509	96.57
0.255	0.010	0.16	0.43	0.178	13.0	0.61	0.177	38.4	2.6	0.00445	96.90
0.26	0.013	0.20	0.435	0.182	13.7	0.62	0.174	39.7	2.7	0.00390	97.21
0.265	0.020	0.27	0.44	0.203	14.4	0.63	0.170	40.9	2.8	0.00343	97.47
0.27	0.025	0.34	0.445	0.215	15.1	0.64	0.166	42.1	2.9	0.00303	97.72
0.275	0.022	0.43	0.45	0.220	15.9	0.65	0.162	43.3	3.0	0.00268	97.90
0.28	0.024	0.51	0.455	0.219	16.7	0.66	0.159	44.5	3.1	0.00230	98.08
0.285	0.034	0.62	0.46	0.216	17.5	0.67	0.155	45.6	3.2	0.00214	98.24
0.29	0.052	0.77	0.465	0.215	18.2	0.68	0.151	46.7	3.3	0.00191	98.39
0.295	0.063	0.98	0.47	0.217	19.0	0.69	0.148	47.8	3.4	0.00171	98.52
0.30	0.061	1.23	0.475	0.220	19.8	0.70	0.144	48.8	3.5	0.00153	98.63
0.305	0.067	1.43	0.48	0.216	20.6	0.71	0.141	49.8	3.6	0.00139	98.74
0.31	0.076	1.69	0.485	0.203	21.3	0.72	0.137	50.8	3.7	0.00125	98.83
0.315	0.082	1.97	0.49	0.199	22.0	0.73	0.134	51.8	3.8	0.00114	98.91
0.32	0.085	2.26	0.495	0.204	22.8	0.74	0.130	52.7	3.9	0.00103	98.99
0.325	0.102	2.60	0.50	0.198	23.5	0.75	0.127	53.7	4.0	0.00095	99.05
0.33	0.115	3.02	0.505	0.197	24.2	0.80	0.1127	57.9	4.1	0.00087	99.13
0.335	0.111	3.40	0.51	0.196	24.9	0.85	0.1003	61.7	4.2	0.00080	99.18
0.34	0.111	3.80	0.515	0.189	25.6	0.90	0.0895	65.1	4.3	0.00073	99.23
0.345	0.117	4.21	0.52	0.187	26.3	0.95	0.0803	68.1	4.4	0.00067	99.29
0.35	0.118	4.63	0.525	0.192	26.9	1.0	0.0725	70.9	4.5	0.00061	99.33
0.355	0.116	5.04	0.53	0.195	27.6	1.1	0.0606	75.7	4.6	0.00056	99.38
0.36	0.116	5.47	0.535	0.197	28.3	1.2	0.0501	79.6	4.7	0.00051	99.41
0.365	0.129	5.89	0.54	0.198	29.0	1.3	0.0406	82.9	4.8	0.00048	99.45
0.37	0.133	6.36	0.545	0.198	29.8	1.4	0.0328	85.5	4.9	0.00044	99.48
0.375	0.132	6.84	0.55	0.195	30.5	1.5	0.0267	87.6	5.0	0.00042	99.51
0.38	0.123	7.29	0.555	0.192	31.2	1.6	0.0220	89.4	6.0	0.00021	99.74
0.385	0.115	7.72	0.56	0.190	31.8	1.7	0.0182	90.83	7.0	0.00012	99.86
0.39	0.112	8.13	0.565	0.189	32.5	1.8	0.0152	92.03			